Diffusion of nonequilibrium carriers in low-dimensional structures

A. Achoyan and S. Petrosyan
Russian-Armenian State University, Yerevan 375051, Armenia

H. E. Ruda and A. Shik
Centre for Advanced Nanotechnology, University of Toronto, Toronto, Canada M5S 3E4

(Received 19 October 2007; published 6 February 2008)

The spatial distribution of nonequilibrium carriers generated by a partial illumination of one- and two-dimensional structures was analyzed theoretically. Due to weak electron screening, the carrier distribution in low-dimensional systems has distinct new features. For monopolar excitation, the concentration of nonequilibrium carriers decreases inside the dark regions hyperbolically in two-dimensional and logarithmically in one-dimensional structures, which results in monopolar injection, barely observable in bulk samples. Bipolar diffusion also differs markedly from that in bulk samples; in particular, there is a long-range hyperbolic tail in the majority carrier distribution, which can be either positive or negative, depending on the mobility ratio of majority and minority carriers.

DOI: 10.1103/PhysRevB.77.085303 PACS number(s): 73.50.Pz, 73.50.Gr

I. INTRODUCTION

The problem of spatial distribution of nonequilibrium carriers in partially or nonuniformly illuminated structures plays a central role in the theory of photoelectric phenomena (see, e.g., Ref. 1). A physical description of the problem and the character of the carrier distribution are different for monopolar and bipolar excitations. The first case, corresponding, for example, to impurity excitation or interband excitation when one type of carriers has a very low mobility, is characterized by a quasiequilibrium (Fermi or Boltzmann) distribution of carriers $\Delta n(\mathbf{r})$ in a self-consistent potential formed by the ionized impurities (or low-mobility carriers) and by $\Delta n(\mathbf{r})$ itself. This distribution is found from the corresponding Poisson equation, and its characteristic spatial extent is of the order of the semiconductor screening radius r_s because screening effects prevent charge separation at larger distances. For bipolar interband excitation and comparable mobilities of both types of the carriers, nonequilibrium electrons and holes may diffuse jointly to quite large distances, so that generation and recombination of carriers occur at different places, and a stationary flux of nonequilibrium carriers exists under illumination. In this case, $\Delta n(\mathbf{r})$ is essentially nonequilibrium and is found from the continuity equation, which usually is solved under the assumption of quasineutrality. Though this equation does not explicitly contain electrostatic forces, actually they play a key role since the concept of quasineutrality assumes that even a small imbalance between the electron and hole concentrations creates a strong electric field acting to restore quasineutrality. To be more exact, the profiles of nonequilibrium electrons and holes do not coincide absolutely but are shifted at the screening radius r_s which in bulk samples is typically much less than the ambipolar diffusion length L.[1] This strong inequality justifies the assumption of local quasineutrality—the basis of standard theory of bipolar diffusion.

In general, Coulomb effects, caused by spatial separation of nonequilibrium carriers, always play an important role and are responsible for the serious distinction in carrier distributions between the cases of monopolar and bipolar excitations.

All of the above-mentioned arguments are applicable to bulk semiconductor samples with all dimensions exceeding r_s. In two-dimensional (2D) layers with thickness $d \ll r_s$, screening effects are much weaker (see, e.g., Refs. 2 and 3) and deviations from local neutrality can be much more noticeable than in bulk samples. In this case the screening length can be comparable or larger than the diffusion length and assumption of local quasineutrality as a rule is not valid. It may essentially change all electronic properties caused by the sample illumination. In one-dimensional (1D) nanowires, the screening effects are suppressed more strongly than in 2D systems,[4] so that the above-mentioned changes should be even more dramatic. Theoretical analysis of the diffusion-drift distribution of nonequilibrium carriers in both 2D and 1D semiconductor structures is the main goal of the present work.

From the formal point of view, the basic difference between bulk and low-dimensional semiconductors consists in the principally different approach used for the theoretical description of screening phenomena. In bulk semiconductors, all points in the sample where the electric field has a nonzero value, contain free carriers moving in this field and providing effective screening. The resulting distribution of carrier concentration and electrical potential are found from the corresponding Poisson's equation. On the contrary, in 2D and 1D structures, electric fields also exist in the whole surrounding space while free carriers are restricted in their motion to a single plane or line, which suppresses dramatically their screening ability. To find the potential distribution in this case, one should solve not the Poisson's but the Laplace equation in the whole space, where charges created by redistribution of nonequilibrium carriers are taken into account in the boundary conditions.

II. TWO-DIMENSIONAL SYSTEMS

A. General expressions

The central goal of the theory of nonequilibrium photoelectric phenomena consists in calculation of the spatial dis-

tribution of the electrical potential φ and the concentrations of nonequilibrium electrons Δn and holes Δp. They should be found from the continuity equations

$$\frac{\partial(\Delta n)}{\partial t} - \nabla \mathbf{j}_n/e = G - R_n, \tag{1}$$

$$\frac{\partial(\Delta p)}{\partial t} + \nabla \mathbf{j}_p/e = G - R_p, \tag{2}$$

$$\mathbf{j}_n = -\sigma_n \nabla \varphi(z=0) + eD_n \nabla(\Delta n), \tag{3}$$

$$\mathbf{j}_p = -\sigma_p \nabla \varphi(z=0) - eD_p \nabla(\Delta p). \tag{4}$$

Here G and $R_{n,p}$ are the generation and recombination rates, and $\sigma_{n,p}$ and $D_{n,p}$ are the electron and hole conductivities and diffusion coefficients. We note that the system contains some amount of equilibrium carriers, which also contribute to recombination, so that, contrary to the generation rate, the electron and hole recombination rates in Eqs. (1) and (2) can be different. We assumed that the 2D electron gas occupies the plane $z=0$. In this case Δn, Δp, as well as the current densities $\mathbf{j}_n$, $\mathbf{j}_p$, are functions of x and y, and all vectors, including the gradient ∇, have only x and y components. As to the potential φ, it depends on all three coordinates but for our purposes only its values and gradient at $z=0$ are relevant. Equations (1)–(4) show no visual distinctions from similar expressions in a bulk sample, but have, in fact, different dimensionalities. In 2D case Δn and Δp are the surface, rather than volume, densities, $\mathbf{j}_n$ and $\mathbf{j}_p$ are the linear current densities (measured, e.g., in the SI unit system in A/m), and $\sigma_{n,p}$ are the 2D conductivities (measured in Ω^{-1} or cm/s, respectively, in SI and Gaussian unit systems).

What is principally different from the bulk case is the connection between the potential and the local charge density, assigned to replace the Poisson's equation. As it was mentioned in Sec. I, it is the Laplace equation $\Delta\varphi=0$, which in our case should be solved in the semispace $z>0$ with the boundary condition (written in the Gaussian system)

$$\frac{\partial\varphi}{\partial z}(z=0) = \frac{2\pi e}{\varepsilon}[\Delta n - \Delta p]. \tag{5}$$

In Eq. (5) we have assumed that our 2D system is embedded into a medium with one single dielectric constant ε, which is typically a good approximation for heterostructures. If the dielectric constants at $z>0$ and $z<0$ differ, say, in the case of a thin film on a dielectric substrate, ε must be replaced by $(\varepsilon_+ + \varepsilon_-)/2$[2]. Equation (5) can be also generalized to the case of metal oxide semiconductor and heterostructures with a metal gate by adding the term describing image forces.

Note that for our theory to be valid, it is not required that both types of carriers are truly 2D with strongly quantized energy spectra in z direction. The only necessary condition is that all characteristic lengths in the xy plane to be obtained from the solution of our equations exceed considerably the electron and hole confinement lengths in z direction. If, besides, electron and holes are separated by the built-in contact electric field at some distance in z direction, this distance must be also much less than the above-mentioned characteristic diffusion lengths.

B. Monopolar excitation

For the case of impurity excitation of electrons, the role of holes is played by empty impurity states, which are immobile ($\sigma_p, D_p=0$), so that $\mathbf{j}_p=0$. As usual (see, e.g., Ref. 5), we present the recombination term in the form $R_n=R_p=R=\gamma_2 np$ where γ_2 is the recombination rate, and $n=n_0+\Delta n$ and $p=p_0+\Delta p$ are the total concentrations consisting of equilibrium and light-induced parts. The subscript 2 at the recombination rate (as well as the similar subscript at the absorption coefficient α_2 below) indicates that we deal with a 2D characteristic having different dimensionalities than in bulk samples ($\mathrm{cm}^{-2}\,\mathrm{s}^{-1}$, rather than $\mathrm{cm}^{-3}\,\mathrm{s}^{-1}$). In uniform samples $n_0=p_0$ due to electrical neutrality. For low light intensities when Δn, $\Delta p \ll n_0$ and in the stationary case the condition $G=R$ resulting from Eq. (2) gives

$$\Delta n + \Delta p = \frac{\alpha_2 I}{\gamma_2 n_0}, \tag{6}$$

where I is the light intensity and α_2 is the absorption coefficient, which in the 2D case is dimensionless (the term $\gamma_2 n_0 p_0$ is exactly compensated by the thermal generation term in G). The same condition applied to Eq. (1) gives $\mathbf{j}_n=\mathrm{const}(\mathbf{r})$. In the open circuit conditions (later we return to this assumption considering the problem of photocurrent) it means simply $\mathbf{j}_n=0$ or, which is the same, quasiequilibrium Fermi distribution of electrons in the potential field $\varphi(x,y,z=0)$ which at $\Delta n \ll n_0$ can be linearized and written in the form $\Delta n(x,y) = e\left(\frac{\partial n_0}{\partial \zeta}\right) \varphi(x,y,z=0) \equiv \varepsilon\varphi(x,y,z=0)/(2\pi e r_2)$ where n_0 is the equilibrium surface concentration of electrons with the chemical potential ζ, and r_2 can be considered as the screening length for 2D electrons.

We consider the carrier distribution in a semi-illuminated sample where the optical excitation occurs only at $x<0$ while the $x>0$ region is dark. In this case Δn and Δp depend only on x, and the boundary condition (5) acquires the form

$$\frac{\partial\varphi}{\partial z}(z=0) = \begin{cases} \dfrac{2\varphi(z=0)}{r_2} - \dfrac{2\pi e\alpha_2 I}{\varepsilon\gamma_2 n_0}, & x<0 \\ \dfrac{2\varphi(z=0)}{r_2}, & x>0. \end{cases} \tag{7}$$

A similar problem arises in the theory of contact phenomena in 2D electron gas,[6] and using these results, we can write the following final answer:

$$\Delta n(x) = \frac{\varepsilon\varphi(x,z=0)}{2\pi e r_2} = \frac{\alpha_2 I}{4\gamma_2 n_0}\left[1 - \frac{4}{\pi}\int_0^\infty \frac{\sin(\xi x/r_2)\,d\xi}{\xi(\xi+2)}\right]. \tag{8}$$

As in most 2D screening problems (see, e.g., Ref. 3), the surface charge far from the boundary $x=0$ decreases very slowly, $\sim|x|^{-1}$. This is the most significant distinction with the similar problem in bulk materials where the density of

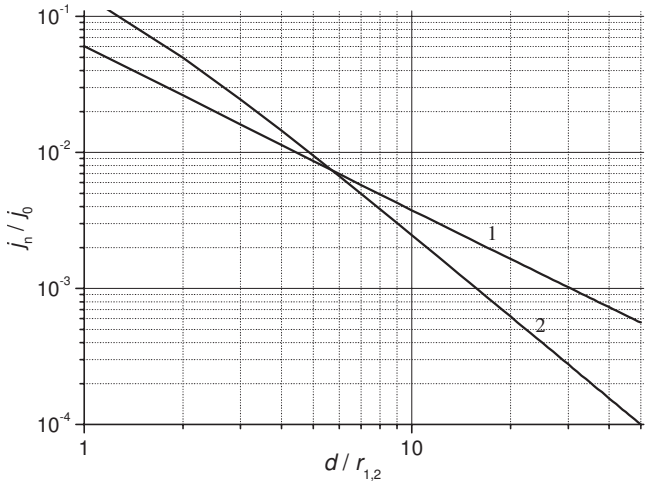

FIG. 1. Current of monopolar injection j_n versus the thickness of nonilluminated region d in one-dimensional (1) and two-dimensional (2) structures. j_n is measured in the units of $j_0 = \frac{\alpha_2 I e D_n}{\pi \gamma_2 n_0 r_{1,2}}$ (note that α_i, γ_i, n_0, j_0, and j_n have different dimensionalities in 1D and 2D systems).

nonequilibrium carriers at monopolar excitation decreases exponentially so that the carriers cannot penetrate into the dark region at the depth exceeding the Debye screening radius r_s.

The slow decrease of $\Delta n(x)$ in the nonilluminated region (monopolar injection) may result in a noticeable monopolar photoconductivity in a sample with only partially illuminated intercontact space—the effect practically unobservable in bulk materials. To consider it theoretically, we assume that the sample we discussed above is provided with the contacts one of which is far inside the illuminated region (at $x \to -\infty$) while the other one occupies the region $x > d > 0$. As it was shown in the beginning of the section, $j_n = \text{const}(x)$ but in the present case this constant is nonzero. Integration of Eq. (3) gives $\sigma_n \varphi(z=0) - eD_n \Delta n + j_n x = \text{const}$ and, introducing a new variable $\Phi(x,z) = \varphi(x,z) + j_n x / \sigma_n$, we find for $\Phi(x,z)$ the same equation as earlier for $\varphi(x,z)$. After solving this with the additional boundary condition $\Delta n(d) = 0$, we finally obtain

$$j_n = -\frac{\alpha_2 I e D_n}{\pi \gamma_2 n_0 r_2} \int_0^\infty \frac{\cos(\xi d / r_2) d\xi}{\xi + 2}. \tag{9}$$

The same result can be obtained if we take into account that under the short circuit conditions, there is no electric field at the contact: $\frac{\partial \varphi}{\partial x}(x=d) = 0$, so that $j_n = eD_n \frac{\partial \Delta n}{\partial x}(d)$, and take $\Delta n(d)$ from Eq. (8). The integral in Eq. (9) diverges at $d \to 0$ since in this limit the condition $\Delta n = 0$ becomes inadequate resulting in infinite concentration gradient. At $d \gg r_2$, the integral is equal to $(r_2/2d)^2$, giving $j_n \sim d^{-2}$ (Fig. 1, curve 2), in agreement with the hyperbolic decrease of $\Delta n(x)$, since the diffusion current is determined by $d(\Delta n)/dx$ at $x = d$, which is proportional to d^{-2}.

Let us discuss the kinetics of charge relaxation after the illumination offset. It is determined by three consecutive generation-recombination and diffusion-drift processes: activation of excess electrons from impurity levels at $x > 0$ (in our formalism they correspond to negative Δp), their transport toward the interface $x = 0$, and capture by excess empty impurity levels at $x < 0$. The reduced dimensionality essentially modifies only the second diffusion-drift process which, due to a large spatial extension of Δn, becomes much slower than in bulk materials. To describe the transport of nonequilibrium electrons, we will take into account only the drift components of current neglecting the diffusion one, as it is always done in the theory of Maxwell relaxation and its 2D analog.[7] For $\Delta n \ll n_0$, Eqs. (1) and (3) result in the equation

$$\frac{\partial(\Delta n)}{\partial t} = -\frac{\sigma_n}{e} \frac{\partial^2 \varphi(z=0)}{\partial x^2}. \tag{10}$$

If the drift transport described by Eq. (10) is the slowest of all three above-mentioned processes responsible for the charge relaxation (or if the impurity levels in the nonilluminated region are absent at all), then electrons in the conduction band and on the impurity levels are in quasiequilibrium, which allows us to assume $\Delta p = -\Delta n$ [given by Eq. (6) in the absence of illumination] in the right side of Eq. (5). The general solution of the Laplace equation with this boundary condition has the form

$$\varphi(x, z \geq 0) = -\frac{8e}{\varepsilon} \int_0^\infty \frac{\sin(\lambda x) \exp(-\lambda z) \tilde{n}(\lambda) d\lambda}{\lambda}, \tag{11}$$

where $\tilde{n}(\lambda) = \int_0^\infty \Delta n(x) \sin(\lambda x) dx$ is the Fourier transform of Δn. Substitution of Eq. (11) into Eq. (10) followed by the Fourier transform results in the equation $\frac{\partial \tilde{n}}{\partial t} = -\frac{4\pi\sigma_n}{\varepsilon} \lambda \tilde{n}$ with the solution

$$\tilde{n}(\lambda, t) = \tilde{n}(\lambda, 0) \exp\left(-\frac{4\pi\sigma_n}{\varepsilon} \lambda t \right).$$

Determining $\tilde{n}(\lambda, 0)$ from Eq. (8), we get the final formula describing relaxation of concentration in the region $x > 0$ as follows:

$$\Delta n(x,t) = \frac{\alpha_2 I}{2\pi\gamma_2 n_0} \int_0^\infty \frac{\sin(\lambda x) \exp(-4\pi\sigma_n \lambda t / \varepsilon) d\lambda}{\lambda + 2/r_2}. \tag{12}$$

Time evolution of the concentration profile $\Delta n(x,t)$ is shown in Fig. 2(a). Since the relaxation consists in the drift-caused returning of nonequilibrium carriers into the region $x < 0$, it begins with fast removal of carriers from the regions close to the illuminated region edge $x = 0$, so that the Δn vs x dependence represents a curve with a maximum gradually moving to higher x. Assuming in Eq. (12) $\partial \Delta n / \partial x = 0$, we obtain the equation for the position of this maximum x_0 as follows:

$$\int_0^\infty \frac{\xi \cos(\xi x_0 / r_2) \exp(-\xi t / \tau_2) d\xi}{\xi + 2} = 0, \tag{13}$$

where $\tau_2 = \varepsilon r_2 / (4\pi\sigma_n)$. The analysis of Eq. (13) shows that at large $t \gg \tau_2$, x_0 linearly increases with time,

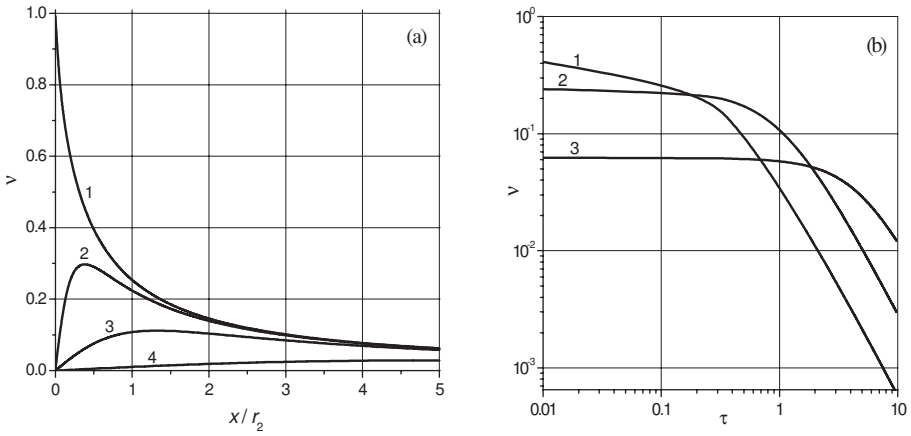

FIG. 2. (a) Coordinate profile of the dimensionless nonequilibrium electron concentration $\nu = \frac{4\gamma_2 n_0}{\alpha I}\Delta n$ in 2D systems at different dimensionless times $\tau = \frac{4\pi\sigma_n}{\varepsilon r_2}t$: (1) $\tau=0$, (2) $\tau=0.2$, (3) $\tau=1$, and (4) $\tau=5$. (b) Relaxation kinetics at (1) $x=0.2r_2$, (2) $x=r_2$, and (3) $x=5r_2$.

$$x_0 \simeq \frac{4\pi\sigma_n}{\varepsilon}t. \tag{14}$$

This is in complete agreement with the known fact that the charge relaxation in 2D systems occurs with a constant velocity $4\pi\sigma_n/\varepsilon$.[7]

Figure 2(b) shows the kinetics of Δn decay at several fixed x. At large t, this function approaches the dependence $\Delta n \sim t^{-2}$.

Another possible situation is realized at low temperatures when the slowest process determining kinetics is the impurity ionization with the characteristic time $\sim\exp(E_i/kT)$ (E_i is the ionization energy). Since this process is independent of the potential distribution in the sample, it does not differ from that in a bulk sample and thus will not be discussed.

C. Bipolar excitation

The properties of nonequilibrium carriers in 2D systems studied in Sec. II B for the case of impurity photoexcitation are essentially modified at interband photoexcitation when screening is provided by both types of mobile carriers—electrons and holes. To analyze these effects we assume, as it is usually done for interband photoexcitation,[5] the linear character of recombination: $R_n=\Delta n/\tau$, $R_p=\Delta p/\tau$. In this case, the system equations (1)–(4) in the stationary case can be reduced to the system

$$\frac{1}{e}(\sigma_n+\sigma_p)\nabla^2\varphi(z=0) - D_n\nabla^2(\Delta n) + D_p\nabla^2(\Delta p) = \frac{1}{\tau}(\Delta p - \Delta n), \tag{15}$$

$$\sigma_p D_n\nabla^2(\Delta n) + \sigma_n D_p\nabla^2(\Delta p) = \frac{1}{\tau}(\sigma_p\Delta n + \sigma_n\Delta p) - G(\sigma_n+\sigma_p). \tag{16}$$

We have linearized the equations neglecting the dependences of $\sigma_{n,p}$ on Δn and Δp.

The problem can be solved relatively simple for strongly extrinsic systems with electron and hole conductivities differing markedly, for example, at $\sigma_n \gg \sigma_p$. In this case Eq. (16) gives

$$D_p\nabla^2(\Delta p) = \frac{\Delta p}{\tau} - G, \tag{17}$$

which means that the minority carrier motion is not influenced by Coulomb forces and comprises a pure diffusion with the coefficient D_p. In the case of semi-illuminated sample: $G=G_0$ at $x<0$; $G=0$ at $x>0$,

$$\Delta p(x) = G_0\tau\left[1 - \tfrac{1}{2}\exp(x/L_p)\right], \quad x<0,$$

$$\Delta p(x) = \frac{G_0\tau}{2}\exp(-x/L_p), \quad x>0, \tag{18}$$

where $L_p=\sqrt{D_p\tau}$.

Then the distributions of a surface charge $q=e(\Delta p-\Delta n)$ and of an electrostatic potential $\varphi(z=0)$ can be found. If we take into account that $\varphi(z=0)$ is connected with q by the expression similar to Eq. (11), than for a planar hole distribution depending on one coordinate x [given, e.g., by Eq. (18)], Eq. (15) gives

$$D_n q''(x) - \frac{q(x)}{\tau} - \frac{4\sigma_n}{\varepsilon}\int_0^\infty \lambda\sin(\lambda x)\int_0^\infty q(t)\sin(\lambda t)dtd\lambda = e(D_n-D_p)(\Delta p(x))'', \tag{19}$$

where $\Delta p(x)$ is given by Eq. (18). Since the right side of Eq. (19) is odd in x, then $q(x)$ also should be odd. Multiplying Eq. (19) by $\sin(\mu x)$ and integrating over x, we obtain the equation for $\tilde{q}(\kappa)=\int_0^\infty q(x)\sin\left(\frac{\kappa x}{L_n}\right)\frac{dx}{L_n}$ as follows:

$$\tilde{q}(\kappa)(\kappa^2+2A\kappa+1) = -\frac{eG_0\tau(1-b)\kappa}{2(1+b\kappa^2)}, \tag{20}$$

which after the inverse Fourier transform gives

$$q(x) = -\frac{eG_0\tau(1-b)}{\pi}\int_0^\infty \frac{\kappa\sin(\kappa x/L_n)d\kappa}{(\kappa^2+2A\kappa+1)(b\kappa^2+1)}. \tag{21}$$

Here $A=\pi\sigma_n\tau/(\varepsilon L_n)$, $L_n=\sqrt{D_n\tau}$, $b=D_p/D_n$.

The spatial distribution of nonequilibrium charge density $q(x)$ depends on the parameters b and A. The first of them characterizes asymmetry of the electron-hole system, which causes the emerging of all electrostatic phenomena discussed in this paper. At $b=1$ both electrons and holes are distributed

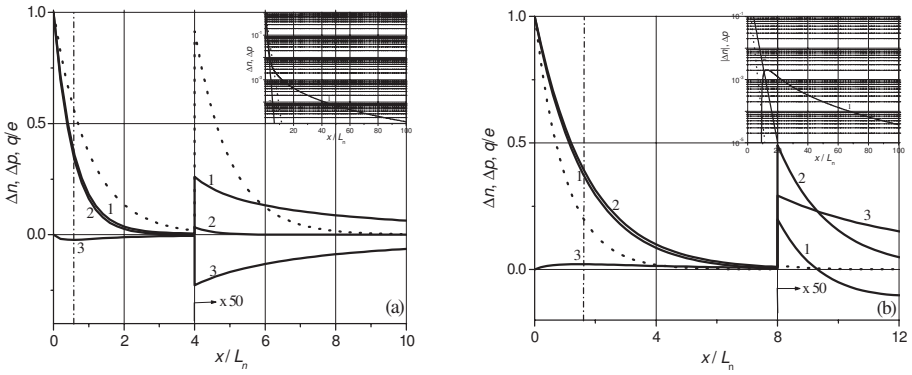

FIG. 3. Spatial distribution of the electron concentration Δn (1), the hole concentration Δp (2), and the surface charge $q=e(\Delta p-\Delta n)$ (3) created by bipolar injection from illuminated region at $A=10$ for $b=0.3$ (a) and $b=3$ (b) in 2D systems. The dotted line shows the dependence $\Delta n \sim \exp(-x/L_n)$. At $x>4L_n$ (a) or $x>8L_n$ (b) the vertical scale is increased. Δn, Δp, and q/e are measured in the units $eG_0\tau$. Vertical dash-and-dot lines show the value of L_p. The inserts show the same concentration profiles in a semilogarithmic scale. Since in the case (b) Δn at large x is positive, the curve 1 at the corresponding insert shows $|\Delta n|$.

in accordance with Eq. (18), local neutrality is maintained, and no difference with bulk samples occurs. At $b<1$ electrons are more mobile than holes, so that $q(x)$ is negative in the nonilluminated region $x>0$ and positive at $x<0$. At $b>1$ the picture is opposite.

The exact shape of distribution is determined by A, which characterizes the relative intensity of drift and diffusion transport. At $A \ll 1$ carrier drift is of a minor importance, so that $q(x)$ at $x>0$ is a superposition of the hole density given by Eq. (18) and the similar expression for the electron density as follows:

$$q(x) = \frac{eG_0\tau}{2}[\exp(-x/L_p) - \exp(-x/L_n)]. \tag{22}$$

At $A \gg 1$ the decay of $\Delta n(x)$ and $q(x)$ is strongly modified by Coulomb effects, which is illustrated by Fig. 3. At relatively small x, the spatial distribution of electrons for any b almost coincides with that of holes, similarly to the bulk samples. However, the tail of electron and charge distribution is essentially different from the three-dimensional case and depends on the value of b.

For $b<1$ (majority carriers are more mobile) the concentration of nonequilibrium electrons at large x decays much slower than the exponential function $\exp(-x/L_n)$. Such a tail, which is seen especially clear at the insert in Fig. 3(a), is reminiscent of hyperbolic charge tails occurring in other 2D electrostatic problems (see Sec. II B and references therein) and has the same physical origin. For $b>1$ (minority carriers are more mobile) the long-range tail has a positive, rather than negative, charge and is caused by removal of some amount of equilibrium electrons.

The mentioned features differing from the characteristics of bipolar diffusion in bulk materials are related to the specific properties of electric potential created by a planar charge distribution. Simple calculations show that two neighboring coplanar stripes of positive and negative surface charges create, contrary to the bulk double charged layer, a nonmonotonic potential distribution shown schematically in Fig. 4. While the spatial distribution of minority carriers (holes) is fixed and given by Eq. (18), the distribution of nonequilibrium electrons is determined by the joint influence of diffusion and drift in the above-mentioned potential. The direction of this drift is shown by arrows in Fig. 4 and explains the observed deviations of $\Delta n(x)$ from the exponential distribution $\exp(-x/L_n)$ shown for comparison by dotted lines in Fig. 3. These deviations include the conforming of $\Delta n(x)$ with $\Delta p(x)$ at small x and long tails at large x caused by accumulation (at $b<1$) or extraction (at $b>1$) of electrons by the self-consistent electric field.

Let us consider the relaxation of the described bipolar carrier distribution after turning off the light excitation. Similarly to the stationary case considered above, the equation for minority carriers splits off and gives

$$\frac{\partial(\Delta p)}{\partial t} = D_p \nabla^2(\Delta p) - \frac{\Delta p}{\tau}. \tag{23}$$

Its solution for the initial condition (18) is

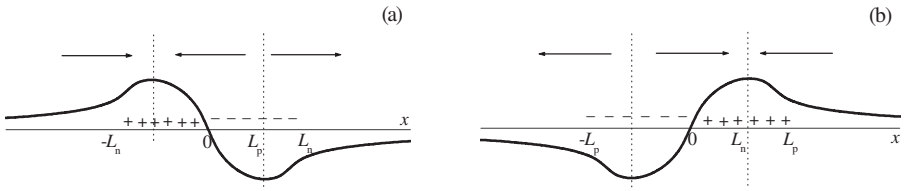

FIG. 4. Schematic distribution of the electrical potential in a 2D layer with bipolar injection for $b<1$ (a) and $b>1$ (b). Pluses and minuses near the axis show the surface charge sign in the given region. Arrows show the direction of electron drift.

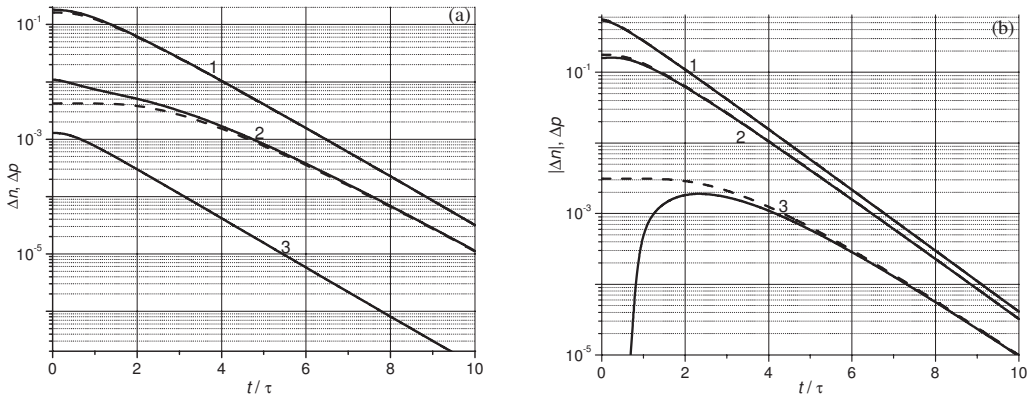

FIG. 5. Relaxation kinetics of electrons (solid lines) and holes (dashed lines) at $A=10$ for $b=0.3$ (a) and $b=3$ (b) in 2D systems at (1) $x=L_n$, (2) $x=3L_n$, and (3) $x=10L_n$. For $b<1$ the value of Δp at $x=10L_n$ is too small and the corresponding curve lies beyond the graph.

$$\Delta p(x,t)=\frac{G_0\tau}{2}\left\{\exp\left(-\frac{t}{\tau}\right)-\frac{2}{\pi}\int_0^\infty \sin\left(\frac{\lambda x}{L_p}\right)\times\exp\left[-\frac{(1+\lambda^2)t}{\tau}\right]\frac{d\lambda}{\lambda(1+\lambda^2)}\right\}. \tag{24}$$

Similarly, the nonstationary analog of Eq. (19) has the form

$$D_n\frac{\partial^2 q(x,t)}{\partial x^2}-\frac{\partial q(x,t)}{\partial t}-\frac{q(x,t)}{\tau}-\frac{4\sigma_n}{\varepsilon}\int_0^\infty \lambda\sin(\lambda x)\int_0^\infty q(\xi,t)\sin(\lambda\xi)d\xi d\lambda=e(D_n-D_p)\frac{\partial^2[\Delta p(x,t)]}{\partial x^2}. \tag{25}$$

Substituting Eq. (24) into the right side of Eq. (25), we obtain the equation for $\tilde{q}(\kappa,t)=\int_0^\infty q(x,t)\sin\left(\frac{\kappa x}{L_n}\right)\frac{dx}{L_n}$ as follows:

$$\tilde{q}(\kappa,t)(\kappa^2+2A\kappa+1)=-\tau\frac{\partial\tilde{q}(\kappa,t)}{\partial t}-\frac{eG_0\tau(1-b)\kappa}{2(1+b\kappa^2)}\times\exp\left[-\frac{(1+b\kappa^2)t}{\tau}\right], \tag{26}$$

generalizing Eq. (20) to the nonstationary case. Equation (26) can be easily solved using $\tilde{q}(\kappa)$ determined by Eq. (20) as the initial condition $\tilde{q}(\kappa,0)$. The inverse Fourier transform gives the final expression for kinetics of the charge distribution

$$q(x,t)=-\frac{eG_0\tau(1-b)}{\pi}\left\{\int_0^\infty\frac{\sin(\kappa x/L_n)\exp\left[-\frac{(1+b\kappa^2)t}{\tau}\right]d\kappa}{[(1-b)\kappa+2A](b\kappa^2+1)}-\int_0^\infty\frac{\sin(\kappa x/L_n)\exp\left[-\frac{(\kappa^2+2A\kappa+1)t}{\tau}\right]d\kappa}{[(1-b)\kappa+2A](\kappa^2+2A\kappa+1)}\right\}. \tag{27}$$

Figure 5(a) shows the relaxation kinetics of Δp [given by Eq. (24)] and Δn [obtained from Eqs. (24) and (27)] in three different points of a sample for the case $b<1$ (majority carriers have higher mobility). At small x (curves 1) where quasineutrality is maintained, electrons and holes relax synchronously. At intermediate x (curves 2), Δp remains almost constant during the initial decay of Δn until these concentrations match, after which their relaxation continues synchronously. Finally, at large x belonging to a long tail of Δn, the concentration of holes is negligibly small, so that we can speak of individual relaxation of Δn. For this reason, Fig. 5(a) has no dashed curve 3 at all since the corresponding dimensionless Δp at $x=10L_n$ even at the initial moment has the order of 10^{-8}. In the case $b>1$ [Fig. 5(b)] the most remarkable feature of the long tail is the change of sign of Δn in the course of relaxation.

III. ONE-DIMENSIONAL SYSTEMS

A. General expressions

In this section we discuss the mono- and bipolar diffusions of carriers in 1D systems (nanowires or nanotubes) assumed to be oriented along the z axis and having radius a.

The main expressions for current equations (1)–(4) given in Sec. II A remain valid in the 1D case as well. The difference consists only in different dimensionalities of the basic characteristics. $\mathbf{j}_{n,p}$ now mean not current densities but currents and, being directed only along z, can be considered as scalars; Δn and Δp are the linear densities of electrons and holes; ∇ in this case means the derivative d/dz. The potential φ in the 1D case is a function of ρ and z, where ρ is the distance from the nanowire axis, and must be found from the Laplace equation in the region $\rho>a$. The fundamental difference between the 1D and 2D cases consists in the expression connecting the potential and the carrier densities and serving as a boundary condition for this equation. In 1D systems, Eq. (5) must be replaced by

$$\frac{\partial\varphi}{\partial\rho}(\rho=a)=\frac{2e(\Delta n-\Delta p)}{\varepsilon a}. \tag{28}$$

Now we use this approach for analyzing the processes of 1D monopolar and bipolar diffusions, similar to those considered in Sec. II for 2D systems.

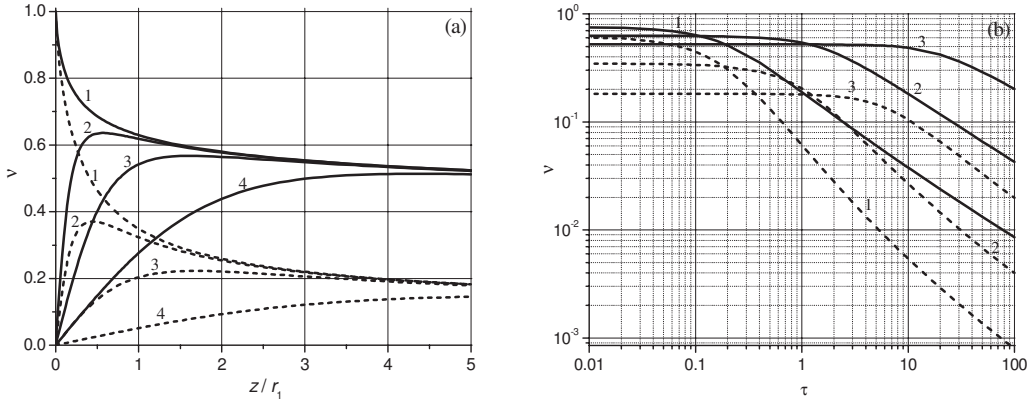

FIG. 6. (a) Coordinate profile of the dimensionless nonequilibrium electron concentration $\nu=\frac{4\gamma_1 n_0}{\alpha_1 I}\Delta n$ in 1D systems at different dimensionless times $\tau=\frac{4\sigma_n}{\varepsilon r_1 a}t$: (1) $\tau=0$, (2) $\tau=0.2$, (3) $\tau=1$, and (4) $\tau=5$. (b) Relaxation kinetics at (1) $x=0.2r_1$, (2) $x=r_1$, and (3) $x=5r_1$. Decay of nonequilibrium electron concentration in nanowires with $a/r_1=0.1$ (solid lines) and $a/r_1=1$ (dashed lines).

B. Monopolar excitation

To consider monopolar injection from the illuminated area $z<0$, we use an analog of Eq. (6) with the quadratic recombination coefficient replaced by γ_1 and the absorption coefficient α_1 to emphasize the difference in dimensionality. Using Eqs. (6) and (28), and the same linearization procedure as in Sec. II B, we obtain a 1D analog of Eq. (7) as follows:

$$\frac{\partial\varphi}{\partial\rho}(\rho=a;z)=\begin{cases}\dfrac{2\varphi(z=0)}{r_1}-\dfrac{2e\alpha_1 I}{\varepsilon a\gamma_1 n_0}, & z<0\\ \dfrac{2\varphi(z=0)}{r_1}, & z>0,\end{cases} \tag{29}$$

where $r_1=\left(\frac{2e^2}{\varepsilon a}\frac{\partial n_0}{\partial\zeta}\right)^{-1}$. The solution of the Laplace equation with this boundary condition is

$$\Delta n(z)=\frac{\varepsilon a\varphi(x,z=0)}{2er_1}=\frac{\alpha_1 I}{4\gamma_1 n_0}\left\{1-\frac{4}{\pi}\int_0^\infty\frac{\sin(\lambda z)d\lambda}{\lambda[2+\lambda r_1 \mathrm{K}_1(\lambda a)/\mathrm{K}_0(\lambda a)]}\right\}, \tag{30}$$

where K_0 and K_1 are the modified Bessel functions. As shown in Fig. 6, the spatial decay of Δn has an extremely slow, logarithmlike character, which is similar to the 1D electrostatic problems considered earlier.[4,8–10] In other words, in 1D systems electrostatic effects do not prevent monopolar injection at macroscopic distances.

If, by analogy with Eq. (9), we consider the diode structure with a metallic contact at the distance d from the illuminated region, the photocurrent j_n will drop with d. We noted in Sec. II B that exact calculation of j_n by solving the Laplace equation with proper boundary conditions gives the same results as a direct application of the simple formula $j_n=eD_n\frac{\partial\Delta n}{\partial z}(d)$. In our case, when $\Delta n(z)$ is given by Eq. (30), it gives

$$j_n=-\frac{\alpha_1 IeD_n}{\pi\gamma_1 n_0 r_1}\int_0^\infty\frac{\cos(\xi d/r_2)d\xi}{2+\xi\mathrm{K}_1(\xi a/r_1)/\mathrm{K}_0(\xi a/r_1)}. \tag{31}$$

The j_n versus d dependence characterizing monopolar injection in 1D system is shown by the curve 1 at Fig. 1. One can see that the current drops with d almost hyperbolically, slower than in the 2D case (curve 2).

If we consider kinetics of nonequilibrium charge relaxation, using the same approach as in Sec. II B, we get, instead of Eq. (12),

$$\Delta n(z,t)=\frac{\alpha_1 I r_1}{4\gamma_1 n_0}\int_0^\infty\frac{\sin(\lambda z)\mathrm{K}_1(\lambda a)}{2\mathrm{K}_0(\lambda a)+\lambda r_1\mathrm{K}_1(\lambda a)}\times\exp\left[-\frac{4\sigma_n\lambda\mathrm{K}_0(\lambda a)}{\varepsilon a\mathrm{K}_1(\lambda a)}t\right]d\lambda. \tag{32}$$

As mentioned in Sec. II B, the analysis of kinetics is based on the continuity equation (10), which neglects the diffusion current in comparison with the drift one. In bulk and 2D systems this is a commonly used approach based on the assumption that the characteristic size of concentration nonuniformity exceeds the Debye screening radius. In 1D systems the situation is different. As shown in Refs. 4 and 7, in nanowires these two current components may be comparable and, moreover, are described by similar diffusion equations where the role of the effective diffusion coefficient in the drift equation is played by $D_1\equiv 2r_1\sigma_n/(\varepsilon a)$. That is why we can easily include the diffusion current $eD_n\nabla n$ in our consideration by simply replacing σ_n in Eq. (32) with the effective conductivity $\sigma^{eff}=\sigma_n+\varepsilon D_n a/(2r_1)$.

Basic characteristics of the monopolar kinetics described by Eq. (32) are illustrated by Fig. 6. They qualitatively resemble Fig. 2 but are characterized by another propagation law for the concentration maximum. The position of this maximum z_0 is determined by z differentiation of Eq. (32) and is found from the equation

$$\int_0^\infty\frac{\xi\cos(\xi)\mathrm{K}_1(\xi a/z_0)}{2z_0\mathrm{K}_0(\xi a/z_0)+\xi r_1\mathrm{K}_1(\xi a/z_0)}\exp\left[-\frac{4\sigma_n\xi\mathrm{K}_0(\xi a/z_0)}{\varepsilon a z_0\mathrm{K}_1(\xi a/z_0)}t\right]d\xi=0. \tag{33}$$

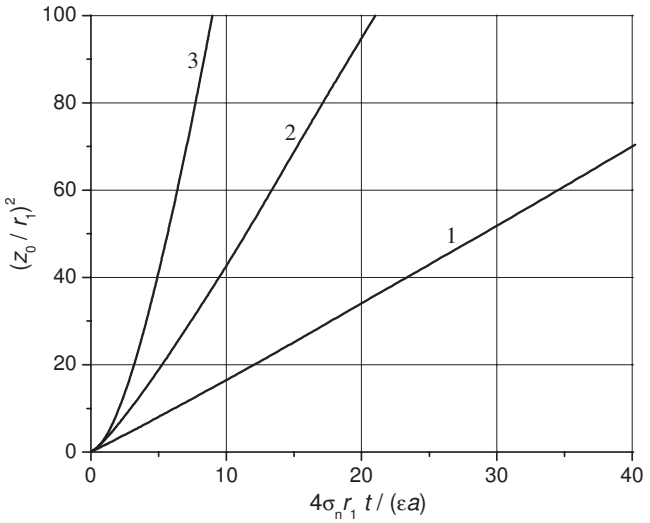

FIG. 7. Time dependence of the nonequilibrium concentration maximum for monopolar injection in 1D systems with (1) $a/r_1=0.01$, (2) $a/r_1=0.1$, and (3) $a/r_1=0.1$.

Determining an analytical relationship between z_0 and t from Eq. (33) proved difficult and hence this operation was performed numerically. The results are presented in Fig. 7. It is seen that this relationship has approximately quadratic character: $z_0^2 \sim D_1 t$, in accordance with the above-mentioned similarity between the drift and diffusion effects in 1D systems and contrary to the linear x_0 versus t connection in 2D systems [Eq. (14)].

C. Bipolar excitation

As we have already mentioned, the difference between diffusion effects in 1D and 2D systems is related exclusively to the different character of electron screening. That is why under conditions of bipolar transport, the distribution of minority carriers, not influenced by electrostatic phenomena, is described with the same equation (18), as in the 2D case (with x replaced by z). Using Eq. (28), we obtain, instead of Eq. (20), the following equation for $\tilde{q}(\kappa)=\int_0^\infty q(z)\sin\left(\frac{\kappa z}{L_n}\right)\frac{dz}{L_n}$:

$$\tilde{q}(\kappa)\left[\kappa^2 + 2A_1\kappa\frac{K_0(\kappa a/L_n)}{K_1(\kappa a/L_n)} + 1\right] = -\frac{eG_0\tau(1-b)\kappa}{2(1+b\kappa^2)}, \tag{34}$$

where $A_1=\sigma_n\tau/(\varepsilon a L_n)$. The inverse Fourier transform results in the formula for $q(z)$ similar to Eq. (21) and differing only by the term containing A_1 (we want to emphasize the difference between A_1 and the 2D parameter A), which contains an additional factor $K_0(\kappa a/L_n)/K_1(\kappa a/L_n)$.

After taking the inverse Fourier transform, we obtain the charge profile $q(z)$ shown in Fig. 8 together with the partial densities of nonequilibrium holes $\Delta p(z)$ [Eq. (18)] and electrons $\Delta n(z)=\Delta p(z)-q(z)/e$. It is characterized by the same qualitative features as the 2D bipolar diffusion discussed in Sec. II C with their essential distinction from the bipolar diffusion in bulk samples.

The kinetics of the bipolar carrier distribution is also similar to the 2D case. The distribution of minority carriers (holes), being not influenced by the arising self-consistent electric field, is given by the same equation (24). The equation for q differs from Eq. (25) only in the term containing A_1, and, instead of Eq. (27), we have eventually

$$q(x,t) = -\frac{eG_0\tau(1-b)}{\pi} \times \left(\int_0^\infty \frac{\sin(\kappa x/L_n)\exp\left[-(1+b\kappa^2)\frac{t}{\tau}\right]d\kappa}{\left[(1-b)\kappa + 2A_1\frac{K_0(\kappa a/L_n)}{K_1(\kappa a/L_n)}\right](b\kappa^2+1)} - \int_0^\infty \frac{\sin(\kappa x/L_n)\exp\left\{-\left[\kappa^2 + 2A_1\frac{K_0(\kappa a/L_n)}{K_1(\kappa a/L_n)}\kappa + 1\right]\frac{t}{\tau}\right\}d\kappa}{\left[(1-b)\kappa + 2A_1\frac{K_0(\kappa a/L_n)}{K_1(\kappa a/L_n)}\right]\left[\kappa^2 + 2A_1\frac{K_0(\kappa a/L_n)}{K_1(\kappa a/L_n)}\kappa + 1\right]} \right). \tag{35}$$

The resulting kinetic curves have no serious distinctions from those for 2D systems shown in Fig. 5. The only difference consists in a shift of the point where Δn changes its sign. For instance, at $x=10L_n$ it occurs at $t \approx 2.1\tau$, contrary to $t \approx 0.6\tau$ for the 2D case [curve 3 in Fig. 5(b)].

IV. CONCLUSIONS

It was shown that in low-dimensional structures, suppression of screening effects due to the confinement of electron motion essentially changes the diffusion processes for a system of injected carriers.

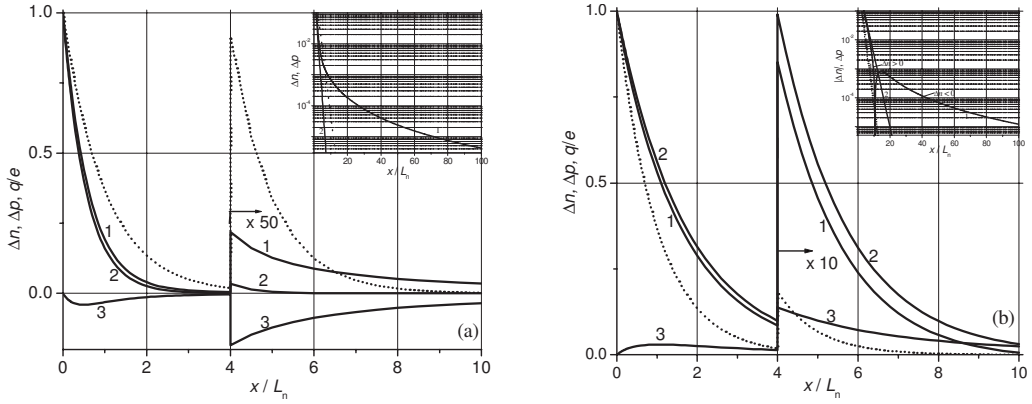

FIG. 8. Spatial distribution of the electron concentration Δn (1), the hole concentration Δp (2), and the surface charge $q=e(\Delta p-\Delta n)$ (3) created by bipolar injection from illuminated region at $A=10$ and $a/L_n=0.1$ for $b=0.3$ (a) and $b=3$ (b) in 1D systems. The dotted line shows the dependence $\Delta n \sim \exp(-x/L_n)$. At $x>4L_n$ the vertical scale is increased. Δn, Δp, and q/e are measured in the units $eG_0\tau$. The inserts show the same concentration profiles in the semilogarithmic scale.

In monopolar diffusion, the density of nonequilibrium carriers decreases inside the dark region very slow, which may result in a new, specifically low-dimensional phenomenon—strong monopolar injection.

In bipolar diffusion, due to a nonmonotonic potential distribution in low-dimensional systems (Fig. 4), drift effects in some cases do not restore but rather destroy quasineutrality. The best demonstration of this phenomenon is the occurrence of a long tail in the distribution of nonequilibrium majority carriers shown in the inserts in Figs. 3 and 8.

ACKNOWLEDGMENTS

Some initial ideas of this paper were formulated long ago in discussions of one of the authors with I. D. Vagner whose untimely death interrupted our common work in this direction. H.E.R. and A.S. also gratefully acknowledge the financial support from NSERC, CIPI, OCE, CSA, and AFOSR in conducting this research. A.A. and S.P. acknowledge the support by Armenian National Program "Semiconductor Nanoelectronics."

[1] T. S. Moss, in *Semiconductors and Semimetals*, edited by R. K. Willardson and A. C. Beer (Academic, New York, 1966), Vol. 2, p. 205.
[2] T. Ando, A. Fowler, and F. Stern, Rev. Mod. Phys. **54**, 437 (1982).
[3] A. Shik, Semiconductors **29**, 697 (1995).
[4] N. S. Averkiev and A. Shik, Semiconductors **30**, 112 (1996).
[5] S. M. Ryvkin, *Photoelectric Effects in Semiconductors* (Consultants Bureau, New York, 1964).
[6] S. G. Petrosyan and A. Y. Shik, Sov. Phys. JETP **69**, 1261 (1989).
[7] M. I. Dyakonov and A. S. Furman, Sov. Phys. JETP **65**, 574 (1987).
[8] F. Leonard and J. Tersoff, Phys. Rev. Lett. **83**, 5174 (1999).
[9] A. A. Odintsov and Y. Tokura, Physica B **284–288**, 1752 (2000).
[10] A. Achoyan, S. Petrosyan, W. Craig, H. E. Ruda, and A. Shik, J. Appl. Phys. **101**, 104308 (2007).